NeuroImage: Clinical 35 (2022) 103097

Contents lists available at ScienceDirect

NeuroImage: Clinical

journal homepage: www.elsevier.com/locate/ynicl

Assessment of intraoperative diffusion EPI distortion and its impact on estimation of supratentorial white matter tract positions in pediatric epilepsy surgery

Joseph Yuan-Mou Yang [a,b,c,d,*,1], Jian Chen [b,1], Bonnie Alexander [a,b], Kurt Schilling [g], Michael Kean [b,d,e], Alison Wray [a,c], Marc Seal [b,d], Wirginia Maixner [a,c,2], Richard Beare [b,f,2]

[a] Department of Neurosurgery, Neuroscience Advanced Clinical Imaging Service (NACIS), The Royal Children's Hospital, Melbourne, Australia
[b] Developmental Imaging, Murdoch Children's Research Institute, Melbourne, Australia
[c] Neuroscience Research, Murdoch Children's Research Institute, Melbourne, Australia
[d] Department of Paediatrics, The University of Melbourne, Melbourne, Australia
[e] Medical Imaging, The Royal Children's Hospital, Melbourne, Australia
[f] Peninsula Clinical School, Faculty of Medicine, Monash University, Melbourne, Australia
[g] Department of Radiology and Radiological Sciences, Vanderbilt University Medical Centre, Nashville, USA

ARTICLE INFO

Keywords:
Intraoperative MRI
Echo planar imaging
Tractography
Diffusion-weighted imaging
Distortion correction
Epilepsy surgery

ABSTRACT

The effectiveness of correcting diffusion Echo Planar Imaging (EPI) distortion and its impact on tractography reconstruction have not been adequately investigated in the intraoperative MRI setting, particularly for High Angular Resolution Diffusion Imaging (HARDI) acquisition. In this study, we evaluated the effectiveness of EPI distortion correction using 27 legacy intraoperative HARDI datasets over two consecutive surgical time points, acquired without reverse phase-encoded data, from 17 children who underwent epilepsy surgery at our institution. The data was processed with EPI distortion correction using the Synb0-Disco technique (Schilling et al., 2019) and without distortion correction. The corrected and uncorrected b0 diffusion-weighted images (DWI) were first compared visually. The mutual information indices between the original T1-weighted images and the fractional anisotropy images derived from corrected and uncorrected DWI were used to quantify the effect of distortion correction. Sixty-four white matter tracts were segmented from each dataset, using a deep-learning based automated tractography algorithm for the purpose of a standardized and unbiased evaluation. Displacement was calculated between tracts generated before and after distortion correction. The tracts were grouped based on their principal morphological orientations to investigate whether the effects of EPI distortion vary with tract orientation. Group differences in tract distortion were investigated both globally, and regionally with respect to proximity to the resecting lesion in the operative hemisphere. Qualitatively, we observed notable improvement in the corrected diffusion images, over the typically affected brain regions near skull-base air sinuses, and correction of additional distortion unique to intraoperative open cranium images, particularly over the resection site. This improvement was supported quantitatively, as mutual information indices between the FA and T1-weighted images were significantly greater after the correction, compared to before the correction. Maximum tract displacement between the corrected and uncorrected data, was in the range of 7.5 to 10.0 mm, a magnitude that would challenge the safety resection margin typically tolerated for tractography-informed surgical guidance. This was particularly relevant for tracts oriented partially or fully in-line with the acquired diffusion phase-encoded direction. Portions of these tracts passing close to the resection site demonstrated significantly greater magnitude of displacement, compared to portions of tracts remote from the resection site in the operative hemisphere. Our findings have direct clinical implication on the accuracy of intraoperative tractography-informed image guidance and emphasize the need to develop a distortion correction technique with feasible intraoperative processing time.

* Corresponding author at: The Royal Children's Hospital, Melbourne, Victoria, Australia.
E-mail address: joseph.yang4@rch.org.au (J.Y.-M. Yang).
[1] Contributed equally for this work.
[2] Joint senior authors for this work.

https://doi.org/10.1016/j.nicl.2022.103097
Received 25 March 2022; Received in revised form 18 May 2022; Accepted 20 June 2022
Available online 23 June 2022

1. Introduction

Open brain surgery is an established treatment with potential to cure children with lesion-based drug-resistant focal epilepsy (Dwivedi et al., 2017; Tellez-Zenteno, Dhar, & Wiebe, 2005). Surgeries performed for lesions located in or adjacent to eloquent cortex and the associated white matter tracts (WMT), have the potential to injure these critical brain structures, leading to permanent postoperative functional deficits with adverse impact on the quality-of-life (Duffau, 2014; Kinoshita et al., 2005). In these surgeries, diffusion magnetic resonance imaging (MRI) tractography provides non-invasive mapping of *in vivo* WMT positions and morphology, that is valuable for presurgical planning and to provide intraoperative image-guidance for safe resection (Essayed et al., 2017; Yang, Yeh, Poupon, & Calamante, 2021). During surgery, the spatial accuracy of preoperatively prepared tractography display is compromised due to the dynamic and progressive brain deformation occurring throughout surgery, also known as intraoperative brain shift, resulting from an interplay of surgical factors, including cerebrospinal fluid loss, brain swelling, and surgical resection (Gerard et al., 2017; Yang et al., 2017). The acquisition of diffusion-weighted intraoperative MRI (iMRI) data allows tractography to be performed intraoperatively and subsequent to intraoperative brain shift, thus facilitating updated tract reconstructions and more accurate surgical guidance and resection (Nimsky et al., 2005; Nimsky, Ganslandt, Merhof, Sorensen, & Fahlbusch, 2006).

In diffusion MRI, the acquisition of diffusion-weighted imaging (DWI) is typically performed using Echo Planar Imaging (EPI) (Ordidge, 1999). The acquisition is usually fast, making it well suited for clinical use. However, due to the low bandwidth in the phase-encode (PE) direction, the diffusion EPI sequence is sensitive to static magnetic field inhomogeneities, resulting in image distortions that are not anatomically faithful to the subject's true anatomy and can be additionally affected by head motion (Jezzard & Balaban, 1995; Jezzard & Clare, 1999). These image distortions tend to occur in regions with an air-tissue interface, such as the orbitofrontal lobe near the ethmoidal and frontal air sinuses, and the temporal pole and basal temporal lobe, near the petrous temporal air sinuses (Jezzard & Balaban, 1995; Jones & Cercignani, 2010). Misalignment between geometrically distorted DWI and anatomical images leads to erroneous local fiber orientation estimates, affecting tractography accuracy over these distorted WM regions (Embleton, Haroon, Morris, Ralph, & Parker, 2010). Studies have shown that correcting diffusion EPI distortion can lead to more accurate and meaningful tractography results for neurosurgery practice (Elliott et al., 2019; Irfanoglu, Walker, Sarlls, Marenco, & Pierpaoli, 2012).

The extent of EPI distortion can be partially mitigated by sequence modification (Frost, Porter, Miller, & Jezzard, 2012; Robson, Anderson, & Gore, 1997), and with parallel imaging (Priest, De Vita, Thomas, & Ordidge, 2006; Schmidt, Degonda, Luechinger, Henke, & Boesiger, 2005) to reduce echo train duration and increase bandwidth. However, this only reduces but does not remove the problem (Jones & Cercignani, 2010).

Methodological development to correct diffusion EPI distortion is an active area of MRI research. Existing techniques can be broadly divided into two classes: a registration-based approach and a field map based approach. The first class uses the undistorted anatomical images, such as the T1-weighted (T1W) and T2-weighted (T2W) images, as the registration template to estimate the degree of distortion (Bhushan, Haldar, Joshi, & Leahy, 2012; Kybic, Thevenaz, Nirkko, & Unser, 2000; Studholme, Constable, & Duncan, 2000; Tao, Fletcher, Gerber, & Whitaker, 2009; Wu et al., 2008). The registration procedure is typically based on image intensity matching between the DWI and the anatomical images. However, the effectiveness of these techniques is heavily dependent on the registration accuracy achieved, and there is also no mechanism to account for image intensity distortion (Hong, To, Teh, Soh, & Chuang, 2015).

The other class of method circumvents the reliance on accurate image registration by estimating the distortion field directly using phase maps (Chen & Wyrwicz, 2001; Jezzard & Balaban, 1995; Reber, Wong, Buxton, & Frank, 1998) or with additionally acquired DWI designed to be sensitized differently to the magnetic susceptibility artifacts, the so-called blip-up blip-down design. The blip-up blip-down based methods, such as FSL TOPUP (Andersson, Skare, & Ashburner, 2003) and TORTOISE (Irfanoglu et al., 2015), require additional b0 image or DWI data acquired with reverse PE direction. The pair of images with same contrast but distortions reversed in directions can then be combined to form a distortion corrected image without loss of information. The corrected DWI output is then used to model and to correct for eddy current distortion using, for example, the FSL Eddy tool (J. L. R. Andersson & Sotiropoulos, 2016). These state-of-the-art, blip-up blip-down based methods are very effective and are widely implemented in diffusion MRI research (Glasser et al., 2013; Gu & Eklund, 2019; Sotiropoulos et al., 2013).

Recently, a hybrid method combing both classes of approaches, called Synb0-DisCo (https://github.com/MASILab/Synb0-DISCO), was proposed (Schilling et al., 2019). It synthesizes an undistorted b0 image from the high resolution T1W image using a deep-learning algorithm. The aim of the synthesis is to create a b0 image with an infinite bandwidth in the PE direction. This undistorted synthetic b0 image is then used as a correction target. The real b0 and the synthetic b0 images form the input to TOPUP, which uses them to estimate the distortion field, thus bypassing the need to acquire reverse PE data. The input to TOPUP overcomes the limitations of registration approaches that do not adequately account for image intensity distortion. The effectiveness of this technique was shown to be comparable to TOPUP and resulted in anatomically faithful geometries when comparing to a high resolution T1W image (Schilling et al., 2020; Schilling et al., 2019). It also allows correction of EPI distortion in legacy DWI data acquired without reverse PE data.

Despite being widely adopted in research, diffusion EPI distortion correction is still not routinely implemented in neurosurgical tractography processing (Albi et al., 2018; Essayed et al., 2017; Ille et al., 2021; Maesawa et al., 2010; Nimsky et al., 2005; Nimsky, Ganslandt, Merhof, Sorensen, & Fahlbusch, 2006; Ostry, Belsan, Otahal, Benes, & Netuka, 2013; Prabhu, Gasco, Tummala, Weinberg, & Rao, 2011; Romano et al., 2011; Shahar et al., 2014). Thus far, investigations have focused on demonstrating the potential impact of EPI distortion on presurgical planning, due to related changes in tumor morphology, and tract spatial displacement, using retrospective adult brain tumor diagnostic MRI data (Albi et al., 2018; Merhof, Soza, Stadlbauer, Greiner, & Nimsky, 2007; Treiber et al., 2016). Evaluation in an intraoperative setting had only been performed in one previous study (Elliott et al., 2019). Questions remained regarding the impact of EPI distortion with intraoperatively acquired High Angular Resolution Diffusion Imaging (HARDI) data that has the potential to optimize tractography reconstruction (Tournier, Mori, & Leemans, 2011; Tuch et al., 2002). There remains a need to systemically evaluate the impact of diffusion EPI distortion on estimating intraoperative WMT positions using iMRI data.

The iMRI data is unique in many ways, such as scans acquired with open cranium, additional imaging artifacts due to the presence of surgical and anesthetic instruments, and brain distortions relating to intraoperative brain shift and surgical resection. These intraoperative factors have potential to complicate the extent and the nature of EPI distortion in different ways, thus pose added challenges, compared to using conventional, closed cranium, presurgical and research MRI data.

Reducing time in surgery is a key surgical risk minimization strategy, and it is thus important to carefully evaluate the benefit-to-time cost of any steps added to a surgical session. Distortion correction increases DWI data preprocessing time and may involve additional data acquisition. It is therefore important to consider whether the improved accuracy justifies the costs in a surgical setting.

In this article, we retrospectively utilized legacy 3Tesla iMRI data acquired without phase reversed data, across two surgical time points,

from 17 children who underwent epilepsy neurosurgery at our institution (Yang et al., 2017). The study aims to: i) evaluate the effectiveness of intraoperative diffusion EPI distortion correction, using the Synb0-DisCo technique; and ii) investigate the effect of distortion correction on estimation of intraoperative tractography positions both globally, and regionally with respect to the tract proximity to the resecting lesion. We explored a range of surgical scenarios for a single iMRI scanner type and provided a framework enabling the evaluation to be carried out for different scanner and sequence combinations.

2. Material and methods

2.1. Patient population

We retrospectively included iMRI data collected from 17 children who underwent open cranial surgery for drug-resistant focal epilepsy at the Royal Children's Hospital (RCH), Melbourne, Australia, between June 2012 to February 2013 (Table 1). They had intra-axial, supratentorial epileptogenic lesions amenable for surgical resection. The data was initially collected for a previous prospective clinical cohort research study, investigating the surgical effects of intraoperative WMT shift (Yang et al., 2017). Both the original and the current studies were approved by the RCH Human Research and Ethics Committee (HREC, approval numbers: 32029 and 72907). Signed, informed consents were obtained from parents or guardians and from cognitively competent older participants for the original study. The RCH HREC approved the subsequent retrospective use of the same iMRI data for this study, as a clinical audit, and determined further informed consent was unnecessary. The participants' clinical and imaging data were de-identified prior to analyses.

2.2. MRI acquisition

The iMRI data was acquired using a 3 Tesla intraoperative MRI scanner (IMRIS Magnetom Verio, Manitoba, Canada) with an eight-channel head coil, and a maximum gradient strength 45 mT/m. Data from two consecutive intraoperative time points were used in this study:

- $iMRI_1$: the pre-resection intraoperative MRI scan, acquired following cranium and dural matter opening, prior to corticectomy and lesion resection, and;
- $iMRI_2$: the post-resection intraoperative MRI scan, acquired following either complete or partial lesion resection, prior to the dura and skull closure.

At each intraoperative time point, a pair of 3D T1W anatomical Magnetization Prepared Rapid Gradient Echo (MPRAGE) sequence (matrix = 256 × 256, FOV = 256, TR = 1800 ms, TE = 2.19 ms, voxels = 1.0 mm^3 isotropic) and a HARDI sequence (60 diffusion weighted directions, 7 b0 volumes, b = 3000 sec/mm^2, TR = 7600 ms, TE = 110 ms, dimension = 104 × 104 × 54, 2.3 mm^3 isotropic voxels) were acquired. The HARDI sequence was acquired with an anterior-to-posterior PE direction, using single shot EPI (SS-EPI).

In all cases, the operative fields were prepared to help minimize the effects of brain shift for intraoperative scan acquisitions. This included filling up the resection cavity with room temperature saline solution, gentle lining and packing of the surgical cavity with saline-soaked surgical patties and cotton balls to prevent surgical cavity collapse and maintain hemostasis, and covering the overlying cortex with wet surgical gauze to prevent drying of the operative field. The dura was left open during the scan. We also ensured that anesthesia was optimized throughout the scan to avoid hypercapnia episodes.

2.3. DWI preprocessing

The DWI preprocessing was performed using the MRtrix3 software (version: 3.0.2–66-g89476794) (Tournier et al., 2019) and the TOPUP and Eddy tools from FSL (fsl-6.0.4) (Jenkinson, Beckmann, Behrens, Woolrich, & Smith, 2012; Smith et al., 2004) incorporated in the MRtrix3 command usage. Fig. 1 summarizes the two versions of DWI preprocessing pipelines, with and without incorporating EPI distortion correction. The DWI data was first denoised using MPPCA (Veraart, Fieremans, & Novikov, 2016a; Veraart et al., 2016b), and then corrected for Gibbs ringing artifacts (Kellner, Dhital, Kiselev, & Reisert, 2016). In the distortion uncorrected pipeline, the DWI was only corrected for motion and eddy current artifacts, using FSL Eddy (Andersson & Sotiropoulos, 2016; Skare & Bammer, 2010). In the distortion corrected pipeline, a TOPUP estimated distortion field map derived as part of running Synb0-DisCo was used to perform the EPI distortion correction (Schilling et al., 2019). The B1 bias field inhomogeneity of all DWI data was corrected for as part of the subsequent fiber orientation distribution (FOD) estimation processing step (see section 2.4). All preprocessed DWI data was co-registered to the participant's T1W image from the corresponding intraoperative time point, using a rigid body transform, so that all subsequent analysis can occur in a common T1W space that aids meaningful surgical interpretation.

The processing time required to estimate distortion field maps using Synb0-DisCo was ~ 40 to 60 minutes per dataset, and running FSL Eddy (eddy_openmp) took another ~ 6 to 8 minutes per dataset, using a CPU workstation with a 16-core processor (AMD Ryzen 9 5950X, 2.20 GHz,

Table 1
Summary of patient demographics, lesion characteristics, histopathology and intraoperative MRI availabilities.

ID	Age (years)	Sex (M/F)	Pathology	Lesion site	$iMRI_1$	$iMRI_2$	Lesion size (ml)
1	13.42	F	Cerebral gliosis (secondary to previous tumor resection)	F	Y		3.9
2	13.42	M	FCD	T	Y	Y	16.5
3	3.75	M	TSC (cortical tuber)	F, T	Y	Y	9.5
4	15.83	M	DNET	F	Y	Y	13.5
5	15.50	M	Presumed Rasmussen encephalitis	F	Y		12.4
6	12.25	M	Cerebral gliosis (secondary to previous tumor resection)	T		Y	20.7
7	4.83	M	FCD	F	Y	Y	3.9
8	10.17	F	Non-specific pathology	T	Y	Y	31.5
9	3.92	F	DNET	TPO	Y	Y	7.3
10	4.17	M	TSC (cortical tuber)	F	Y	Y	7.8
11	3.83	M	FCD	F	Y		76.4
12	4.50	M	FCD	F, T, P, I	Y		163.3
13	10.92	F	DNET	O	Y	Y	7.0
14	13.25	F	DNET	TPO		Y	5.2
15	16.08	M	FCD	F	Y	Y	2.9
16	12.17	F	DNET	TPO	Y	Y	24.2
17	5.05	F	Pilocytic astrocytoma	Thalamus	Y		31.1

Abbreviations: Dysembryoplastic neuroepithelial tumors, DNET; Focal cortical dysplasia, FCD; Tuberous Sclerosis Complex, TSC; Temporal lobe, T, Frontal lobe, F; Parietal lobe, P; Insular cortex, I; Temporo-parieto-occipital junction, TPO; Yes, Y.

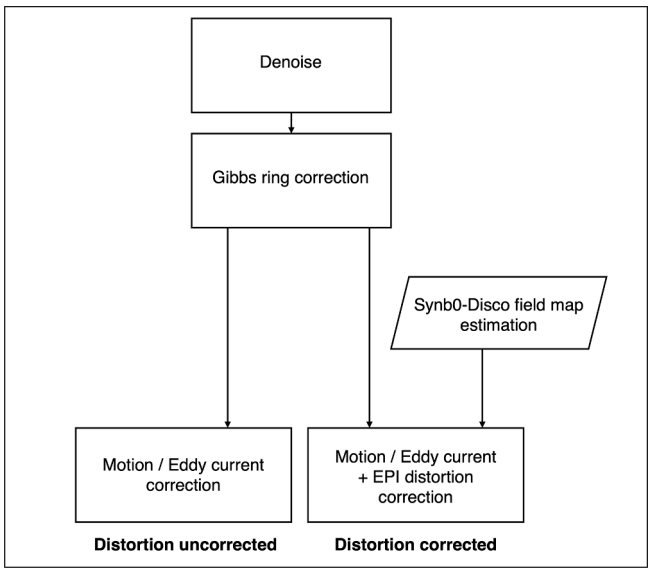

Fig. 1. The DWI data preprocessing flowchart [print as a single image].

max 5.08 GHz, 130G memory).

2.4. WMT bundle segmentation

Seventy-two WMT bundles were segmented from each DWI dataset, using TractSeg, an unsupervised, convolution neural network-based automated WMT segmentation tool (Wasserthal, Neher, & Maier-Hein, 2018). The algorithm was pre-trained on 150 reference WMT segmentations from 105 Human Connectome Project subjects (Sotiropoulos et al., 2013). TractSeg directly segments the tracts in the field of FOD peaks, estimated using the single-shell 3-tissue Constrained Spherical Deconvolution (CSD) model from MRtrix3Tissue, a fork of MRtrix3 (https://3tissue.github.io/, version 3Tissue_v5.2.0) (Dhollander, Raffelt, & Connelly, 2016). The B1 bias field inhomogeneity of the DWI data was corrected as part of the multi-tissue CSD informed log-domain intensity normalization step (Dhollander et al., 2021; Raffelt et al., 2017; Tournier et al., 2019).

The infratentorial brainstem WMTs were excluded from this study given the supratentorial WMTs are the usual surgical focus. We also excluded the fornix, given its known problematic reconstructions in TractSeg (Wasserthal et al., 2018). The remaining 64 segmented WMTs were grouped into five categories according to their principal morphological orientations (Fig. 2): i) anterior-posterior (AP), ii) left–right (LR), iii) C-shaped, iv) inferior-superior, straight (IS-Straight), and v) inferior-superior, oblique (IS-Oblique) oriented tracts. All segmented binarized WMT masks were transformed to the T1W space, using the same DWI to T1 rigid body transform derived previously.

2.5. Lesion segmentation

To enable the lesion proximity analysis (see below), the target lesions were manually segmented by the first author (JYMY), an experienced neurosurgical research fellow, using these patients' preoperative 3D T1W data (MPRAGE, Siemens Magnetom Trio scanner, matrix = 256 × 256, FOV = 250, TR = 1900 ms, TE = 2.69 ms, voxels = 0.8 mm^3 isotropic). The segmented lesion masks were then rigidly transformed and warped to each intraoperative T1W image.

2.6. Data analysis

To address the first study aim (i.e. to evaluate the effectiveness of distortion correction), the DWI data before and after corrections were

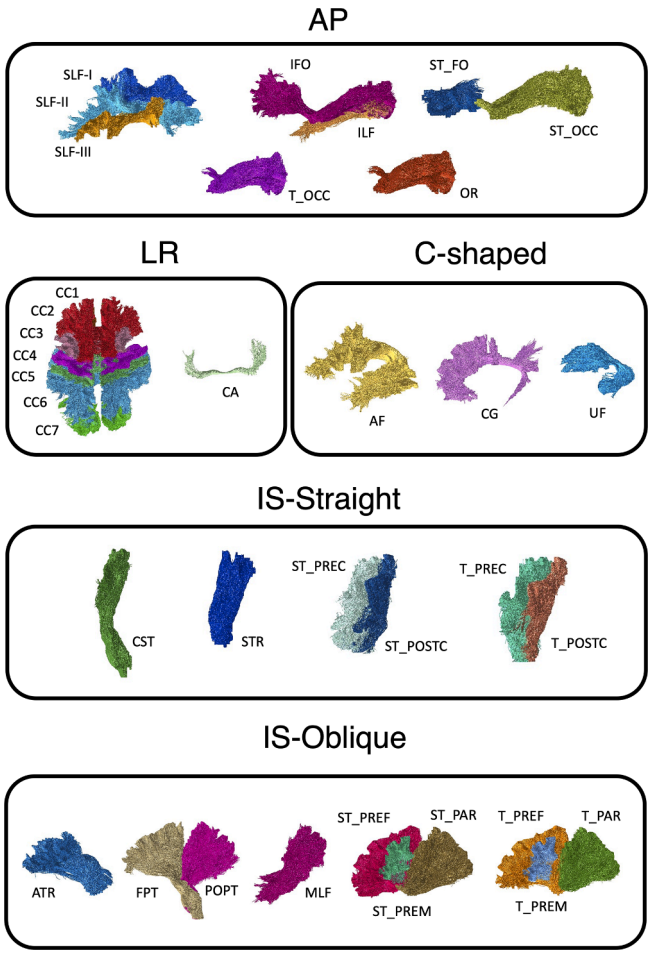

Fig. 2. Selected TractSeg derived white matter tract segmentations used in this study, categorized by their principal morphological orientations. AP (anterior-posterior), LR (left–right), IS-Straight (inferior-superior, straight), IS-Oblique (inferior-superior, oblique), and C-shaped oriented tracts. Abbreviations: Arcuate fascicle, AF; Anterior Thalamic Radiation, ATR; Commissure Anterior, CA; Corpus Callosum, CC (1 = Rostrum; 2 = Genu; 3 = Rostral body [Premotor]; 4 = Anterior midbody [Primary Motor]; 5 = Posterior midbody [Primary Somatosensory]; 6 = Isthmus; 7 = Splenium); Cingulum, CG; Corticospinal tract, CST; Middle longitudinal fascicle, MLF; Fronto-pontine tract, FPT; Inferior occipito-frontal fascicle, IFO; Inferior longitudinal fascicle, ILF; Optic radiation, OR; Parietooccipital pontine tract, POPT; Superior longitudinal fascicle I, SLF-I; Superior longitudinal fascicle II, SLF-II; Superior longitudinal fascicle III, SLF-III; Superior Thalamic Radiation, STR; Uncinate fascicle, UF; T_PREF = Thalamo-prefrontal tract, T_PREF; Thalamo-premotor tract, T_PREM; Thalamo-precentral tract, T_PREC; Thalamo-postcentral tract, T_POSTC; Thalamo-parietal tract, T_PAR; Thalamo-occipital tract, T_OCC; Striato-fronto-orbital tract, ST_FO; Striato-prefrontal tract, ST_PREF; Striato-premotor tract, ST_PREM; Striato-precentral tract, ST_PREC; Striato-postcentral tract, ST_POSTC; Striato-parietal tract, ST_PAR; Striato-occipital tract, ST_OCC. [print as a single image].

visually inspected, looking for any differences in image appearance and geometries. Mattes mutual information (MI) similarity indices (Mattes, Haynor, Vesselle, Lewellyn, & Eubank, 2001) were calculated between the DWI-derived fractional anisotropy (FA) maps, and the corresponding T1W image, using *SimpleITK R* package (Beare, Lowekamp, & Yaniv, 2018). The FA maps were derived by applying diffusion tensor estimation to both the distortion corrected and uncorrected DWI data, using an iterated weighted least-squares approach (Basser, Mattiello, & LeBihan, 1994; Veraart, Sijbers, Sunaert, Leemans, & Jeurissen, 2013). The MI indices were used to quantify the effects of distortion correction in the Synb0-Disco paper (Schilling et al., 2019). The FA maps were used as

registration targets beacuase they are derived from the entire DWI dataset and have tissue contrasts sufficiently similar to T1W images for registration to function effectively.

To address the second study aim (i.e. to investigate the effect of distortion correction on estimation of intraoperative tractography positions), the effect of distortion correction on estimated tract position was investigated by computing the Hausdorff distance between the same WMT derived from distortion corrected and uncorrected DWI. The Hausdorff distance represents the greatest displacement between the two tracts (see Inline Suppl Fig. 2 for an illustrated example). WMTs were grouped for comparison purposes on the bases of morphological orientation with further divisions into sub-groups based on lesion proximity. The lesion proximity grouping allows the magnitude of the lesion effect to be tested. Two lesion proximity thresholds, 5.0 mm and 10.0 mm were used to group tracts within the operative hemisphere – tracts passing closer to the lesion than the threshold (proximal) were compared to the others (remote).

2.7. Statistical analysis

The MI indices calculated from each version of the DWI data were then compared using paired t-tests.

The Hausdorff distances were reported as group means and 95% confidence intervals (CI) based on each WMT morphological orientation category, and separately for the $iMRI_1$ and $iMRI_2$ data.

The Hausdorff distances of lesion proximity sub-groups were compared using a multilevel model with patient ID as a random effect, to account for within-patient clustering of Hausdorff distances. We reported both uncorrected and Bonferroni corrected p-values. Cohen's d was used to represent the effect sizes. A Cohen'd = 0.2, 0.5, and 0.8 is considered as indicating a small, medium, and large effect size, respectively (Cohen, 1992). Statistical significance was defined by a corrected p-value ≤ 0.05.

3. Results

There were 17 participants in total. The $iMRI_1$ data were available in 15 participants, and the $iMRI_2$ data were available in 12 participants. Ten participants had data available at both intraoperative time points.

3.1. Qualitative assessments of the DWI data with and without EPI distortion correction

Fig. 3 and Fig. 4 highlight selected case examples. Compared to no correction, the EPI distortion was visibly improved in the corrected DWI data, notably over the frontal pole, the temporal pole, the basal temporal lobe near the petrous temporal air sinuses, the occipital pole, and the dorsal cerebellar hemisphere near the torcular venous sinuses confluence (i.e. at the brain-blood interface). There were also visible improvements in the image distortion, following correction, at and near the skull pin sites (MRI conditional titanium pins used to fix the head in the operative position), over the exposed cortical surface at the craniotomy site, at the brain-lesion boundaries, and distortion affected the geometry of the lesions, and the surgical cavities.

3.2. Mutual information between the FA and T1W images

The MI similarity indices were significantly greater for the FA maps derived from the distortion corrected DWI, compared to those derived from the uncorrected DWI, at both intraoperative time points (Fig. 5). For the $iMRI_1$ data: the group mean MI based on the distortion corrected DWI = 0.423 ± 0.034 (SD) versus the group mean MI based on the uncorrected DWI = 0.415 ± 0.036 ($p = 1.94 \times 10^{-4}$, Cohen's d = 1.22). For the $iMRI_2$ data: the group mean MI based on the distortion corrected DWI = 0.435 ± 0.036 versus the group mean MI based on the uncorrected DWI = 0.427 ± 0.035 ($p = 2.13 \times 10^{-5}$, Cohen's d = 2.03).

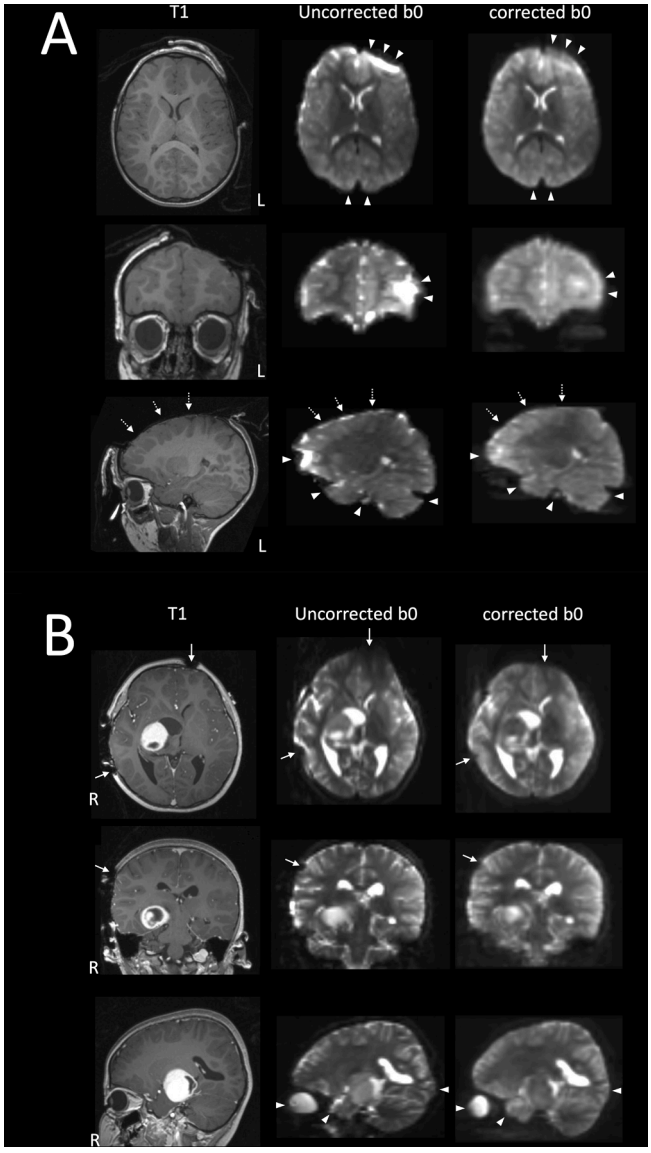

Fig. 3. Two case examples illustrating the quality of DWI-EPI distortion correction using the Synb0-DisCo technique. A: patient 11; B: patient 17. Both intraoperative MRI were acquired at the first surgical stage ($iMRI_1$), following cranial opening, prior to corticectomy and lesion resection. Selected orthogonal T1W images, both distortion corrected and uncorrected b0 images are shown in radiological orientation (left, L; right, R). There are visible improvements in the DWI-EPI distortion post correction, at the typically described basal frontal, temporal and occipital regions, the dorsal cerebellar hemisphere and the globe (white arrowheads). There is additional correction of b0 image distortion at and near the metallic skull pin sites (solid white arrows), and over the exposed cortical surface at the craniotomy site (dashed white arrows). [print as a single image].

3.3. EPI distortion related WMT displacements

3.3.1. The WMT morphological orientation groups

The WMT from the four morphological orientation groups in the operative hemisphere demonstrated consistent patterns and similar magnitudes of displacement at both intraoperative time points (Fig. 6). The difference in the group means of tract displacements measured by Hausdorff distance, derived from the distortion corrected and uncorrected DWI data, ranged between 7.5 mm and 10.0 mm. Displacement of the IS-Straight oriented WMT was lower than the AP, C-shaped and IS-Oblique oriented WMTs. Similar overall displacement patterns were demonstrated globally when accounting for both the operative and the

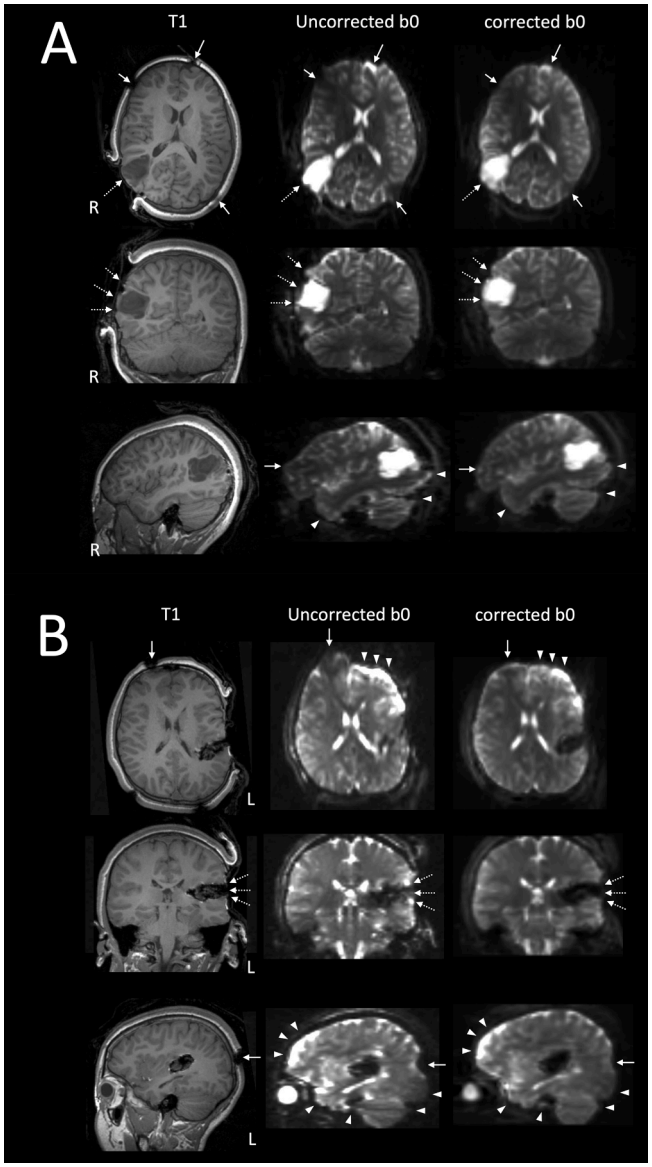

Fig. 4. Two case examples illustrating the quality of DWI-EPI distortion correction using the Synb0-DisCo technique. A: patient 16, the intraoperative MRI was acquired at the first surgical stage ($iMRI_1$), following cranial opening, prior to corticectomy and lesion resection. B: patient 14, the intraoperative MRI data was acquired at the second surgical stage ($iMRI_2$), following initial lesion resection. Selected orthogonal T1W images, both distortion corrected and uncorrected b0 images are shown in radiological orientation (left, L; right, R). Similar to those shown in Fig. 3, distortion corrections were most notable over the typical frontal, temporal and occipital regions (white arrowheads). Additional distortion corrections are again noted at and near the metallic skull pin sites (solid white arrows), over the exposed cortical surface at the craniotomy site, at the brain-lesion boundaries, and affected the geometry of the lesions, and the surgical cavities (dashed white arrows). [print as a single image].

non-operative hemispheres (see Inline Suppl Fig. 1).

3.3.2. *The lesion proximity groups*

Table 2 summarizes the tract-lesion proximity analysis results within the operative hemisphere at both intraoperative time points. There were generally greater amounts of WMT displacement between the distortion corrected and uncorrected DWI data, for tracts passing close to the lesion than those remote from the lesion.

At the first surgical time point ($iMRI_1$), significantly greater displacement was observed in the AP oriented WMT proximal to the lesion for both the 5.0 mm and 10.0 mm thresholds (Bonferroni corrected $p = 0.001$, Cohen's $d = 0.38$; Bonferroni corrected $p = 0.005$, Cohen's $d = 0.35$). Significantly greater displacement was also observed in the IS-Oblique oriented tracts proximal to the lesion for the 10.0 mm threshold (Bonferroni corrected $p = 0.02$, Cohen's $d = 0.24$).

At the second surgical time point ($iMRI_2$), significantly greater displacements were detected for both the AP oriented and IS-Oblique oriented WMT proximal to the lesion for both the 5.0 mm and 10.0 mm thresholds (For AP oriented WMT: Bonferroni corrected $p = 0.01$, Cohen's $d = 0.38$; Bonferroni corrected $p = 0.007$, Cohen's $d = 0.37$; For IS-Oblique oriented WMT: Bonferroni corrected $p = 0.0009$, Cohen's $d = 0.48$; Bonferroni corrected $p = 0.02$, Cohen's $d = 0.36$). Significantly greater displacement was also observed in the IS-Straight oriented tracts proximal to the lesion for the 10.0 mm threshold (Bonferroni corrected $p = 0.009$, Cohen's $d = 0.57$).

4. Discussion

To our knowledge, this is the first study investigating the effectiveness of diffusion EPI distortion correction and its impact on tractography outputs, using intraoperatively acquired HARDI data. In the first part of this study, we evaluated the effectiveness of performing distortion correction using the Synb0-DisCo technique. We demonstrated both qualitatively through data inspection, and quantitatively by the MI indices derived from the FA and T1W images, significant improvements in the anatomical fidelity of the post-correction DWI images, compared to the uncorrected data.

Apart from demonstrating notable distortion correction in the typically described regions containing air-tissue interface, our study additionally revealed distortion correction in other brain areas, unique to the intraoperative condition, an observation also made by a recent iMRI study (Elliott et al., 2019). Specifically, we demonstrated additional anatomical infidelities between the T1W image, and the DWI distortion observed at and near the titanium skull pin sites, over the exposed cortical surface under the craniotomy site, and at the tumor-brain margins/boundaries, with altered geometries noted in the tumor and at the resecting surgical cavities. Such observation implies the distortion must be corrected to achieve meaningful, and arguably more anatomically accurate intraoperative tractography results for use in surgical resection guidance.

Some of the image distortions shown were not solely due to the EPI acquisition. For example, distortion relating to the metallic skull pins is induced by metallic artefact. Distortion correction methods that rely on additional b0 images with reverse PE direction may be suboptimal for this use, because the additional b0 images are themselves susceptible to metallic artefact induced distortion. We presume the anatomical fidelity of the images was much improved after distortion correction because rather than using additional b0 images, the Synb0-DisCo technique utilizes a T1W image to estimate the distortion field. Thus the Synb0-DisCo technique may offer a means to correct such image distortions unique to an intraoperative setting.

In the second part of this study, we characterized the intraoperative WMT displacement between the distortion corrected and uncorrected images, at two different intraoperative time points. The group mean of tract displacements measured by Hausdorff distance from each WMT orientation category was similar, between 7.5 and 10.0 mm. The maximum displacement occurred in WMT oriented either aligned with or containing components oriented in the acquired PE direction (i.e. the AP, IS-Oblique and C-shaped oriented WMT in our study). The distortion was greater for these tracts passing close to the resecting lesion, compared to other tracts remote from the lesion.

To our knowledge, the only other study investigating intraoperative EPI distortion using 3Tesla iMRI data is that by Elliott et al. (2019). The authors tackled the problem of minimizing distortion differently, by comparing performance of two different EPI sequences, as opposed to

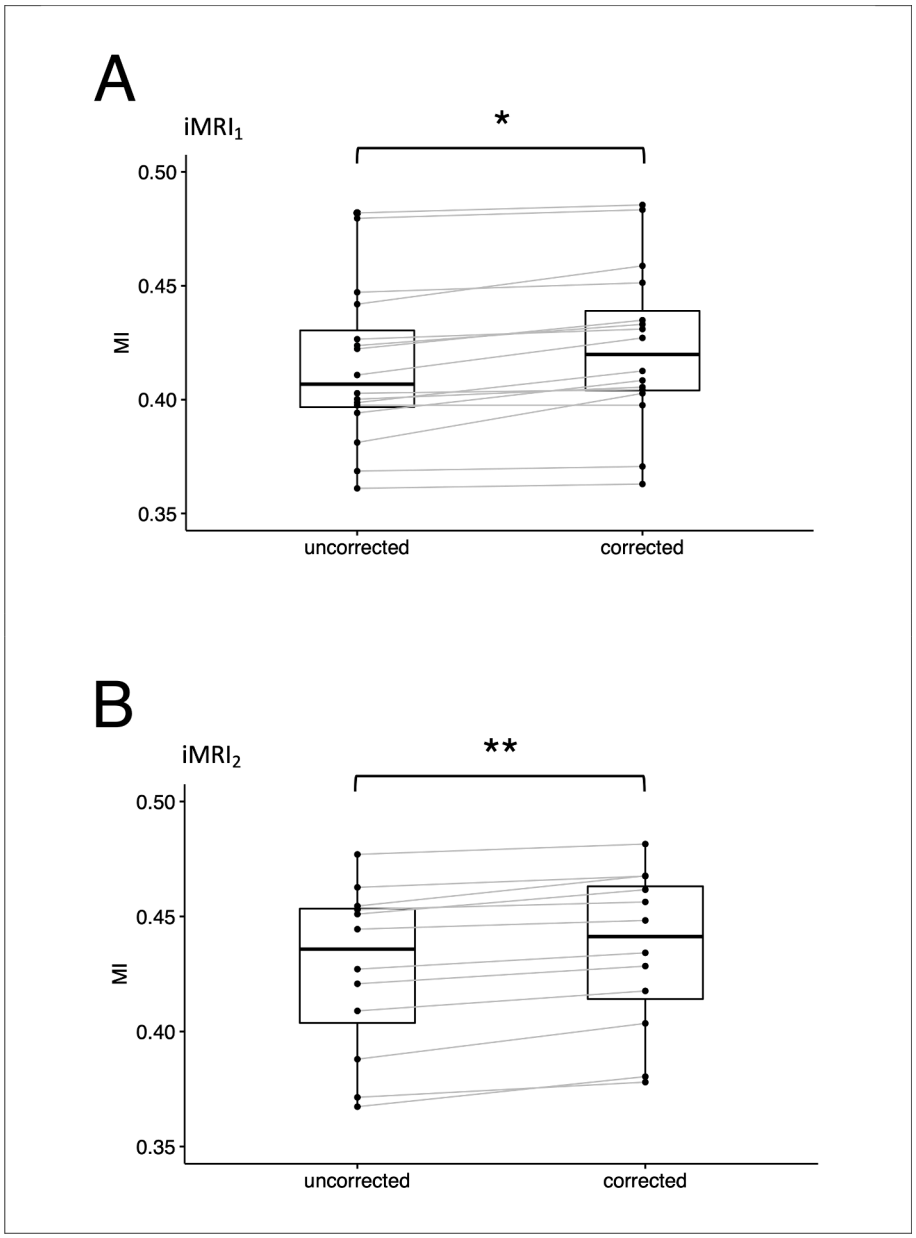

Fig. 5. Mutual information between the FA and T1W images, with and without EPI distortion correction using the Synb0-DisCo technique. A: intraoperative MRI data acquired at the first surgical time point ($iMRI_1$), following cranial opening, prior to corticectomy and lesion resection. B: data acquired at the second surgical time point ($iMRI_2$) following initial lesion resection. The mutual information indices were significantly greater for EPI distortion corrected diffusion data compared to those without correction, at both surgical time points. * $p < 0.001$ ** $p < 0.0001$. Abbreviation: intraoperative magnetic resonance imaging, iMRI; mutual information, MI. [print as a single image].

implementing distortion correction, in data from 22 adult brain tumor patients. The study demonstrated intraoperative diffusion data acquired using a readout segmented EPI (RS-EPI; with shortened echo train) had less regional susceptibility artifact with more anatomical faithful geometries, and permitted more successful tractography reconstruction, than data acquired using a standard SS-EPI. The reported mean inter-sequence tract displacement was 9.5 mm (SD 5.7 mm), similar to our reported maximum tract displacement difference between the corrected and uncorrected data.

Other investigations in healthy participants (Embleton et al., 2010; Irfanoglu et al., 2012; Jones & Cercignani, 2010), and in brain tumor imaging for presurgical planning (Albi et al., 2018; Merhof et al., 2007; Treiber et al., 2016), also demonstrated that EPI distortion can lead to clinically significant inaccuracies in tractography appearance and position. In one study, greater tract mask spatial overlap scores were achieved when distortion was corrected for, between the DWI data acquired in two different and orthogonal PE directions, in the same individuals (Irfanoglu et al., 2012).

4.1. Clinical implications

Collectively, our findings have significant implication for the accuracy of intraoperative tractography-informed image guidance. Surgical resection misinformed by erroneous tracking results can lead to permanent functional damage due to inadvertent injuries to the WMT (Duffau, 2014; Kinoshita et al., 2005). Our EPI acquisition had an anterior-to-posterior PE direction, thus have greater impact on the WMTs partially or fully in-line with this orientation. Notably, the AP oriented tracts include the optic radiation (OR in Fig. 2), reconstructed in anterior temporal tumor and epilepsy surgeries, to map out its anterior temporal component, or the Meyer's loop, for visual field preservation (Cui et al., 2015; Yang et al., 2019); the inferior fronto-occipital fasciculus and inferior longitudinal fasciculus (IFO and ILF in Fig. 2) both as ventral language pathways in surgeries conducted over the dorsolateral frontal lobe, at the temporal stem, the basal temporal lobe and over the dorsolateral occipital lobe and occipital pole (Duffau, 2005, 2008). Other tracts containing AP oriented fibers are also implicated. This included the C-shaped oriented tracts, such as the arcuate fasciculus

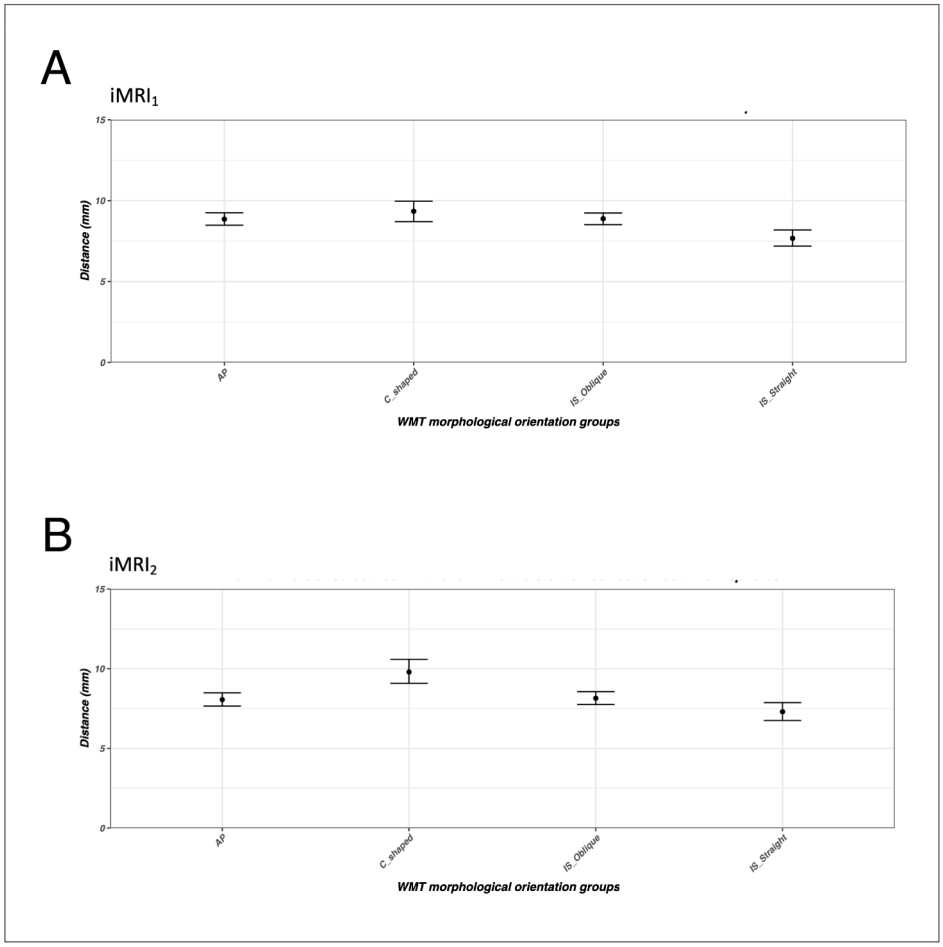

Fig. 6. The group mean and 95% confidence interval of tract displacements measured by Hausdorff distance, between the distortion corrected and uncorrected DWI data, in the operative hemisphere, at intraoperative time points $iMRI_1$ (A) and $iMRI_2$ (B). The solid black circles represent the group means, and the bars represent the 95% confidence interval. Abbreviations: anterior-posterior, AP; inferior-superior, IS; intraoperative magnetic resonance imaging, first surgical time point ($iMRI_1$); intraoperative magnetic resonance imaging, second surgical time point ($iMRI_2$); white matter tract, WMT. [print as a single image].

Table 2
Comparisons of Hausdorff distance by lesion proximity sub-groups and tract orientation in the operative hemisphere, at the two intraoperative time points ($iMRI_1$ and $iMRI_2$).

	WMT Groups	Hausdorff distance (mm)		p	Cohen's d	Corrected p#	Hausdorff distance (mm)		p	Cohen's d	Corrected p#
		Proximal (≤5 mm)	Remote (>5 mm)				Proximal (≤10 mm)	Remote (>10 mm)			
$iMRI_1$	AP	10.12	8.60	0.0003***	0.38	0.001**	9.88	8.59	0.001**	0.35	0.005**
	C-shaped	11.34	9.87	0.12	0.25	0.47	11.46	9.69	0.053	0.31	0.21
	IS-Oblique	9.72	8.62	0.02*	0.21	0.07	9.74	8.51	0.006**	0.24	0.02*
	IS-Straight	9.11	8.22	0.39	0.25	1.00	9.82	7.77	0.02*	0.25	0.08
$iMRI_2$	AP	9.39	8.03	0.003**	0.38	0.01*	9.33	7.98	0.002**	0.37	0.007**
	C-shaped	10.15	10.44	0.80	0.09	1.00	10.58	10.28	0.78	0.09	1.00
	IS-Oblique	9.14	7.84	0.0002***	0.48	0.0009***	8.80	7.86	0.004**	0.36	0.02*
	IS-Straight	8.92	7.54	0.10	0.86	0.40	9.29	7.23	0.002**	0.57	0.009**

Abbreviations: Anterior-Posterior, AP; Inferior-Superior, IS; Intraoperative magnetic resonance imaging, first surgery time point, $iMRI_1$; intraoperative magnetic resonance imaging, second surgery time point, $iMRI_2$; millimeter, mm; White matter tract, WMT. * $p < 0.05$, ** $p < 0.01$,*** $p < 0.001$, #: Bonferroni correction for multiple comparison.

(AF in Fig. 2) for language preservation in language-dominant frontal, parietal and temporal operculum surgeries (Duffau, 2008; Yang et al., 2020); the IS-Oblique oriented tracts, such as the parietal thalamic radiation (T_PAR in Fig. 2) in superior parietal surgery for sensory preservation. The IS-Straight oriented tracts, such as the corticospinal tract (CST in Fig. 2), reconstructed for motor preservation, appeared to be the least impacted, although this finding was limited by small sample size and the small effect sizes observed in the related analyses (Table 2).

The magnitude of maximum WMT displacement between the corrected and uncorrected images identified in this study, especially those passing close to the resecting lesion, challenges the 10.0 mm safety resection margin typically tolerated for surgery guided by preoperative tractography (Berman, Berger, Chung, Nagarajan, & Henry, 2007; Kamada et al., 2005; Mikuni et al., 2007), and ~ 5.0 mm for surgery guided by intraoperatively tractography (Yang et al., 2017). Our findings would advocate further research efforts to develop and to implement diffusion EPI distortion correction methods within the intraoperatively acceptable processing time.

4.2. Limitations

While the adoption of an automated tractography algorithm in this study was chosen to provide methodological standardization, it clearly departs from standard clinical tractography practice utilizing regions-of-interest (ROI) based targeted streamline tractography, and the algorithm does not incorporate any explicit handling of the effects of brain pathology (Wasserthal et al., 2018). Our study took advantage of the algorithm being unsupervised and completely data-driven, automatically generating a large number of WMT, to ensure systematic and unbiased estimation of tract displacement, without introducing bias or variability resulting from manually placed ROIs (Colon-Perez et al., 2016; Schilling et al., 2021). Manually defined ROI utilize a priori anatomical information guided by the T1W images that were warped to each version of the DWI data in our study, thus, the effect of which would be impossible to disentangle from the effect of EPI distortion correction alone.

Other study limitations include that our findings are based on a single high-field iMRI scanner type, small clinical sample size with heterogenous epilepsy history, lesion histopathology, different lesion sizes and locations. The susceptibility artifact may be less pronounced in open cranial surgical field for the low-field (0.5–1.5Tesla) iMRI scanners, although the tradeoff being a lower signal to noise ratio, for example. Further studies using larger clinical datasets with different iMRI scanner types are needed for more comprehensive evaluation. The nature of our legacy DWI data acquired without reverse PE data determined the chosen distortion correction method used in this study. Ideally, we would like to have been able to compare distortion correction using reverse PE images, with correction using Synb0-Disco. However, we consider that this dataset is unique in offering the opportunity to evaluate distortion in as-yet rarely available intraoperative HARDI data, and is valuable in demonstrating the utility of T1-based distortion correction where reverse PE images cannot be acquired. The Synb0-Disco technique was trained on data from healthy adult individuals, not on children and not on iMRI data. A comprehensive evaluation of performance between different state-of-the-art distortion correction techniques is beyond the scope of the current study. Future prospective iMRI studies from larger clinical cohorts are needed in order to better understand the nuances of different correction techniques applied in an intraoperative setting.

Lastly, we prepared the operative field in a manner that minimized the effect of brain shift on intraoperative MRI. It remains unclear what the impact of severe brain shift on EPI distortion will be, and whether the severity of anatomical distortion imposes a limit on the anatomical fidelity of the reconstructed synthetic b0 images from Synb0-Dico. Such questions will need to be addressed with alternative intraoperative MRI datasets acquired under different surgical conditions.

4.3. Future research directions and clinical recommendations

Currently, the processing time required for state-of-art EPI distortion correction techniques, like Synb0-Disco and TOPUP, is incompatible with an intraoperative timeframe. Future advancements in computational hardware and software, and network capacity may eventually overcome this practice bottleneck (Maller, Grieve, Vogrin, & Welton, 2020). Until then, we strongly recommend that neurosurgeons always inspect the intraoperative DWI data themselves, looking for regions of image distortions that do not have anatomical faithful geometries, compared to the T1W images. This should be followed by careful interpretation of subsequent tractography results, in well recognized areas, such as the orbitofrontal lobe and the temporal pole, but also in areas close to the skull pin sites, near the craniotomy cortical surface and critically, at the lesion-brain boundaries relevant for surgical resection. Added care is also needed for surgeries requiring reconstruction of tracts oriented partially or in-line with the acquired PE direction, particularly near the resection margins. We advocate, when appropriate, for validation of tractography results against intraoperative direct brain electrostimulation or intraoperative electrophysiology for functional brain mapping, a surgical gold-standard for confirming the location of functional cortex and the position of the subserving subcortical WMT, nearby the resection site (Berger & Hadjipanayis, 2007; Duffau, 2015). Future research studies investigating effects of EPI distortion on intraoperative tractography should also report such indirect functional validation, to help us better understand the functional relevance of the tractography results (Elliott et al., 2019).

Further exploration of alternative EPI acquisition schemes, such as the multishot EPI and RS-EPI, and parallel imaging, with potential to reduce the severity of EPI geometric distortion, is an active area of research with translation potential in the intraoperative setting (Elliott et al., 2019; Frost et al., 2012; Priest et al., 2006; Robson et al., 1997; Schmidt et al., 2005; Wang et al., 2018). Efforts should also aim to incorporate the acquisition of higher order DWI data, such as HARDI, using these alternative EPI schemes. Utilization of HARDI data will likely lead to improvement in the anatomical accuracy of the intraoperative tractography results.

Lastly, while our study condition was strictly intraoperative, based on our findings together with those from preoperative settings (Albi et al., 2018; Irfanoglu et al., 2012; Merhof et al., 2007; Treiber et al., 2016), and expert opinions (Essayed et al., 2017; Yang et al., 2021;Yeh, Irimia, Bastos, & Golby, 2021), we strongly advocate incorporating EPI distortion correction for all preoperative tractography processing workflows used for presurgical planning. This is particularly imperative in the semi-acute and elective surgical settings where data acquisition and processing time is less of an issue, compared to acute surgical settings. The majority of epilepsy brain surgeries and low-grade brain tumor surgeries would fall under this category. Correction using the Synb0-Disco technique makes use of T1W anatomical data already available in most clinically acquired MRI protocols. Alternatively, acquiring an additional pair of b0 images with reversed PE directions for the TOPUP technique, only adds approximately one extra minute of scanning time.

5. Conclusions

In conclusion, EPI distortion correction using the Synb0-Disco technique, with intraoperatively acquired HARDI data, improves the anatomical fidelity of the diffusion images both qualitatively and quantitatively, compared to the structural images. The maximum erroneous tract displacement derived from the uncorrected data exceeds the safety resection margin typically tolerated for tractography-informed image guidance. This is particularly relevant for surgeries requiring reconstruction of WMT oriented partially or in-line with the acquired PE direction, and for tracts passing close to the resection site. Our findings have direct clinical implications for the accuracy of intraoperative tractography-informed image guidance and emphasize the need to develop a distortion correction technique with feasible intraoperative processing time.

6. Data availability statement

The iMRI data used in this study was acquired from clinical patients. They were not made openly available due to ethics issue of handling clinical data.

CRediT authorship contribution statement

Joseph Yuan-Mou Yang: Conceptualization, Methodology, Validation, Formal analysis, Investigation, Data curation, Writing – original draft, Writing – review & editing, Visualization, Project administration, Funding acquisition. **Jian Chen:** Conceptualization, Methodology, Software, Validation, Formal analysis, Investigation, Data curation, Writing – original draft, Writing – review & editing, Visualization.

Bonnie Alexander: Conceptualization, Methodology, Writing – review & editing, Visualization. **Kurt Schilling:** Resources, Writing – review & editing. **Michael Kean:** Investigation, Resources, Writing – review & editing. **Alison Wray:** Investigation, Resources, Writing – review & editing. **Marc Seal:** Resources, Writing – review & editing. **Wirginia Maixner:** Investigation, Resources, Writing – review & editing, Supervision. **Richard Beare:** Conceptualization, Methodology, Formal analysis, Investigation, Writing – original draft, Writing – review & editing, Supervision.

Acknowledgements

This research was conducted within the Department of Neurosurgery, The Royal Children's Hospital, and the Developmental Imaging Group, Murdoch Children's Research Institute at the Melbourne Children's MRI Centre, Melbourne, Victoria. It was supported by The Royal Children's Hospital Foundation, Murdoch Children's Research Institute, The University of Melbourne, Department of Paediatrics, and the Victorian Government's Operational Infrastructure Support Program.

Disclosure

All authors report no conflict of interests relevant to the manuscript. **Bonnie Alexander**, **Joseph Yuan-Mou Yang** and **Richard Beare** receive positional funding from the Royal Children's Hospital Foundation (RCH 1000). This work received research funding support from The Johnstone Family Foundation.

Appendix A. Supplementary data

Supplementary data to this article can be found online at https://doi.org/10.1016/j.nicl.2022.103097.

References

Albi, A., Meola, A., Zhang, F., Kahali, P., Rigolo, L., Tax, C.M.W., Ciris, P.A., Essayed, W. I., Unadkat, P., Norton, I., Rathi, Y., Olubiyi, O., Golby, A.J., O'Donnell, L.J., 2018. Image Registration to Compensate for EPI Distortion in Patients with Brain Tumors: An Evaluation of Tract-Specific Effects. J. Neuroimaging 28 (2), 173–182.

Andersson, J.L., Skare, S., Ashburner, J., 2003. How to correct susceptibility distortions in spin-echo echo-planar images: application to diffusion tensor imaging. Neuroimage 20 (2), 870–888. https://doi.org/10.1016/S1053-8119(03)00336-7.

Andersson, J.L.R., Sotiropoulos, S.N., 2016. An integrated approach to correction for off-resonance effects and subject movement in diffusion MR imaging. Neuroimage 125, 1063–1078. https://doi.org/10.1016/j.neuroimage.2015.10.019.

Basser, P.J., Mattiello, J., LeBihan, D., 1994. Estimation of the effective self-diffusion tensor from the NMR spin echo. Retrieved from J. Magn. Reson. B 103 (3), 247–254. http://www.ncbi.nlm.nih.gov/entrez/query.fcgi?cmd=Retrieve&db=PubMed&dopt=Citation&list_uids=8019776.

Beare, R., Lowekamp, B., Yaniv, Z., 2018. Image Segmentation, Registration and Characterization in R with SimpleITK. J. Stat. Softw. 86 https://doi.org/10.18637/jss.v086.i08.

Berger, M.S., Hadjipanayis, C.G., 2007. Surgery of intrinsic cerebral tumors. *Neurosurgery, 61*(1 Suppl), 279-304; discussion 304-275. doi:10.1227/01.NEU.0000255489.88321.18.

Berman, J.I., Berger, M.S., Chung, S.W., Nagarajan, S.S., Henry, R.G., 2007. Accuracy of diffusion tensor magnetic resonance imaging tractography assessed using intraoperative subcortical stimulation mapping and magnetic source imaging. J. Neurosurg. 107 (3), 488–494. https://doi.org/10.3171/JNS-07/09/0488.

Bhushan, C., Haldar, J.P., Joshi, A.A., Leahy, R.M., 2012. Correcting Susceptibility-Induced Distortion in Diffusion-Weighted MRI using Constrained Nonrigid Registration. *Signal Inf Process Assoc Annu Summit Conf APSIPA Asia Pac, 2012*. Retrieved from https://www.ncbi.nlm.nih.gov/pubmed/26767197.

Chen, N.K., Wyrwicz, A.M., 2001. Optimized distortion correction technique for echo planar imaging. Magn. Reson. Med. 45 (3), 525–528. https://doi.org/10.1002/1522-2594(200103)45:3<525::aid-mrm1070>3.0.co;2-s.

Cohen, J., 1992. A power primer. Psychol. Bull. 112 (1), 155–159. https://doi.org/10.1037//0033-2909.112.1.155.

Colon-Perez, L.M., Triplett, W., Bohsali, A., Corti, M., Nguyen, P.T., Patten, C., Mareci, T. H., Price, C.C., 2016. A majority rule approach for region-of-interest-guided streamline fiber tractography. Brain Imaging Behav. 10 (4), 1137–1147.

Cui, Z., Ling, Z., Pan, L., Song, H., Chen, X., Shi, W., . . . Luan, G., 2015. Optic radiation mapping reduces the risk of visual field deficits in anterior temporal lobe resection. Int. J. Clin. Exp. Med., *8*(8), 14283-14295. Retrieved from https://www.ncbi.nlm.nih.gov/pubmed/26550412.

Dhollander, T., Raffelt, D., Connelly, A., 2016. Unsupervised 3-tissue response function estimation from single-shell or multi-shell diffusion MR data without a co-registered T1 image. Paper presented at the ISMRM Workshop on Breaking the Barriers of Diffusion MRI Lisbon, Portugal.

Dhollander, T., Tabbara, R., Rosnarho-Tornstrand, J., Tournier, J.D., Raffelt, D., Connelly, A., 2021. Multi-tissue log-domain intensity and inhomogeneity normalisation for quantitative apparent fibre density. Paper presented at the Proc. ISMRM 29, 2472.

Duffau, H., 2005. Lessons from brain mapping in surgery for low-grade glioma: insights into associations between tumour and brain plasticity. Lancet Neurol. 4 (8), 476–486. https://doi.org/10.1016/S1474-4422(05)70140-X.

Duffau, H., 2008. The anatomo-functional connectivity of language revisited. New insights provided by electrostimulation and tractography. Neuropsychologia 46 (4), 927–934. https://doi.org/10.1016/j.neuropsychologia.2007.10.025.

Duffau, H., 2014. The dangers of magnetic resonance imaging diffusion tensor tractography in brain surgery. World Neurosurg. 81 (1), 56–58. https://doi.org/10.1016/j.wneu.2013.01.116.

Duffau, H., 2015. Stimulation mapping of white matter tracts to study brain functional connectivity. Nat. Rev. Neurol. 11 (5), 255–265. https://doi.org/10.1038/nrneurol.2015.51.

Dwivedi, R., Ramanujam, B., Chandra, P.S., Sapra, S., Gulati, S., Kalaivani, M., Garg, A., Bal, C.S., Tripathi, M., Dwivedi, S.N., Sagar, R., Sarkar, C., Tripathi, M., 2017. Surgery for Drug-Resistant Epilepsy in Children. N. Engl. J. Med. 377 (17), 1639–1647.

Elliott, C.A., Danyluk, H., Aronyk, K.E., Au, K., Wheatley, B.M., Gross, D.W., Sankar, T., Beaulieu, C., 2019. Intraoperative acquisition of DTI in cranial neurosurgery: readout-segmented DTI versus standard single-shot DTI. J. Neurosurg. 1–10. https://doi.org/10.3171/2019.5.JNS19890.

Embleton, K.V., Haroon, H.A., Morris, D.M., Ralph, M.A., Parker, G.J., 2010. Distortion correction for diffusion-weighted MRI tractography and fMRI in the temporal lobes. Hum. Brain Mapp. 31 (10), 1570–1587. https://doi.org/10.1002/hbm.20959.

Essayed, W.I., Zhang, F., Unadkat, P., Cosgrove, G.R., Golby, A.J., O'Donnell, L.J., 2017. White matter tractography for neurosurgical planning: A topography-based review of the current state of the art. Neuroimage Clin 15, 659–672. https://doi.org/10.1016/j.nicl.2017.06.011.

Frost, R., Porter, D.A., Miller, K.L., Jezzard, P., 2012. Implementation and assessment of diffusion-weighted partial Fourier readout-segmented echo-planar imaging. Magn. Reson. Med. 68 (2), 441–451. https://doi.org/10.1002/mrm.23242.

Gerard, I.J., Kersten-Oertel, M., Petrecca, K., Sirhan, D., Hall, J.A., Collins, D.L., 2017. Brain shift in neuronavigation of brain tumors: A review. Med. Image Anal. 35, 403–420. https://doi.org/10.1016/j.media.2016.08.007.

Glasser, M.F., Sotiropoulos, S.N., Wilson, J.A., Coalson, T.S., Fischl, B., Andersson, J.L., Xu, J., Jbabdi, S., Webster, M., Polimeni, J.R., Van Essen, D.C., Jenkinson, M., 2013. The minimal preprocessing pipelines for the Human Connectome Project. Neuroimage 80, 105–124.

Gu, X., Eklund, A., 2019. Evaluation of Six Phase Encoding Based Susceptibility Distortion Correction Methods for Diffusion MRI. Front Neuroinform 13, 76. https://doi.org/10.3389/fninf.2019.00076.

Hong, X., To, X.V., Teh, I., Soh, J.R., Chuang, K.H., 2015. Evaluation of EPI distortion correction methods for quantitative MRI of the brain at high magnetic field. Magn. Reson. Imaging 33 (9), 1098–1105. https://doi.org/10.1016/j.mri.2015.06.010.

Ille, S., Schroeder, A., Wagner, A., Negwer, C., Kreiser, K., Meyer, B., Krieg, S.M., 2021. Intraoperative MRI-based elastic fusion for anatomically accurate tractography of the corticospinal tract: correlation with intraoperative neuromonitoring and clinical status. Neurosurg. Focus 50 (1), E9. https://doi.org/10.3171/2020.10.FOCUS20774.

Irfanoglu, M.O., Modi, P., Nayak, A., Hutchinson, E.B., Sarlls, J., Pierpaoli, C., 2015. DR-BUDDI (Diffeomorphic Registration for Blip-Up blip-Down Diffusion Imaging) method for correcting echo planar imaging distortions. Neuroimage 106, 284–299. https://doi.org/10.1016/j.neuroimage.2014.11.042.

Irfanoglu, M.O., Walker, L., Sarlls, J., Marenco, S., Pierpaoli, C., 2012. Effects of image distortions originating from susceptibility variations and concomitant fields on diffusion MRI tractography results. Neuroimage 61 (1), 275–288. https://doi.org/10.1016/j.neuroimage.2012.02.054.

Jenkinson, M., Beckmann, C.F., Behrens, T.E.J., Woolrich, M.W., Smith, S.M., 2012. FSL. Fsl. Neuroimage 62 (2), 782–790.

Jezzard, P., Balaban, R.S., 1995. Correction for geometric distortion in echo planar images from B0 field variations. Magn. Reson. Med. 34 (1), 65–73. https://doi.org/10.1002/mrm.1910340111.

Jezzard, P., Clare, S., 1999. Sources of distortion in functional MRI data. Hum. Brain Mapp. 8 (2–3), 80–85. https://doi.org/10.1002/(sici)1097-0193(1999)8:2/3<80::aid-hbm2>3.0.co;2-c.

Jones, D.K., Cercignani, M., 2010. Twenty-five pitfalls in the analysis of diffusion MRI data. NMR Biomed. 23 (7), 803–820. https://doi.org/10.1002/nbm.1543.

Kamada, K., Todo, T., Masutani, Y., Aoki, S., Ino, K., Takano, T., Kirino, T., Kawahara, N., Morita, A., 2005. Combined use of tractography-integrated functional neuronavigation and direct fiber stimulation. J. Neurosurg. 102 (4), 664–672.

Kellner, E., Dhital, B., Kiselev, V.G., Reisert, M., 2016. Gibbs-ringing artifact removal based on local subvoxel-shifts. Magn. Reson. Med. 76 (5), 1574–1581. https://doi.org/10.1002/mrm.26054.

Kinoshita, M., Yamada, K., Hashimoto, N., Kato, A., Izumoto, S., Baba, T., Maruno, M., Nishimura, T., Yoshimine, T., 2005. Fiber-tracking does not accurately estimate size of fiber bundle in pathological condition: initial neurosurgical experience using neuronavigation and subcortical white matter stimulation. Neuroimage 25 (2), 424–429.

Kybic, J., Thevenaz, P., Nirkko, A., Unser, M., 2000. Unwarping of unidirectionally distorted EPI images. IEEE Trans. Med. Imaging 19 (2), 80–93. https://doi.org/10.1109/42.836368.

Maesawa, S., Fujii, M., Nakahara, N., Watanabe, T., Wakabayashi, T., Yoshida, J., 2010. Intraoperative tractography and motor evoked potential (MEP) monitoring in surgery for gliomas around the corticospinal tract. World Neurosurg. 74 (1), 153–161. https://doi.org/10.1016/j.wneu.2010.03.022.

Maller, J.J., Grieve, S.M., Vogrin, S.J., Welton, T., 2020. Performance gains with Compute Unified Device Architecture-enabled eddy current correction for diffusion MRI. NeuroReport 31 (10), 746–753. https://doi.org/10.1097/WNR.0000000000001475.

Mattes, D., Haynor, D.R., Vesselle, H., Lewellyn, T.K., Eubank, W., 2001. Nonrigid multimodality image registration. Paper presented at the Proc. SPIE 4322, Medical Imaging 2001: Image Processing.

Merhof, D., Soza, G., Stadlbauer, A., Greiner, G., Nimsky, C., 2007. Correction of susceptibility artifacts in diffusion tensor data using non-linear registration. Med. Image Anal. 11 (6), 588–603. https://doi.org/10.1016/j.media.2007.05.004.

Mikuni, N., Okada, T., Enatsu, R., Miki, Y., Hanakawa, T., Urayama, S.-I., Kikuta, K., Takahashi, J.A., Nozaki, K., Fukuyama, H., Hashimoto, N., 2007. Clinical impact of integrated functional neuronavigation and subcortical electrical stimulation to preserve motor function during resection of brain tumors. J. Neurosurg. 106 (4), 593–598.

Nimsky, C., Ganslandt, O., Hastreiter, P., Wang, R., Benner, T., Sorensen, A.G., Fahlbusch, R., 2005. Intraoperative diffusion-tensor MR imaging: shifting of white matter tracts during neurosurgical procedures–initial experience. Radiology 234 (1), 218–225. https://doi.org/10.1148/radiol.2341031984.

Nimsky, C., Ganslandt, O., Merhof, D., Sorensen, A.G., Fahlbusch, R., 2006. Intraoperative visualization of the pyramidal tract by diffusion-tensor-imaging-based fiber tracking. Neuroimage 30 (4), 1219–1229. https://doi.org/10.1016/j.neuroimage.2005.11.001.

Ordidge, R., 1999. The development of echo-planar imaging (EPI): 1977-1982. *MAGMA, 9*(3), 117-121. Retrieved from https://www.ncbi.nlm.nih.gov/pubmed/10628684.

Ostry, S., Belsan, T., Otahal, J., Benes, V., & Netuka, D. (2013). Is intraoperative diffusion tensor imaging at 3.0T comparable to subcortical corticospinal tract mapping? Neurosurgery, 73(5), 797-807; discussion 806-797. doi:10.1227/NEU.0000000000000087.

Prabhu, S.S., Gasco, J., Tummala, S., Weinberg, J.S., Rao, G., 2011. Intraoperative magnetic resonance imaging-guided tractography with integrated monopolar subcortical functional mapping for resection of brain tumors. Clinical article. J. Neurosurg. 114 (3), 719–726. https://doi.org/10.3171/2010.9.JNS10481.

Priest, A.N., De Vita, E., Thomas, D.L., Ordidge, R.J., 2006. EPI distortion correction from a simultaneously acquired distortion map using TRAIL. J. Magn. Reson. Imaging 23 (4), 597–603. https://doi.org/10.1002/jmri.20508.

Raffelt, D., Dhollander, T., Tournier, J.D., Tabbara, R., Smith, R.E., Pierre, E., Connelly, A., 2017. Bias Field Correction and Intensity Normalisation for Quantitative Analysis of Apparent Fibre Density. Paper presented at the Proc. ISMRM 26, 3541.

Reber, P.J., Wong, E.C., Buxton, R.B., Frank, L.R., 1998. Correction of off resonance-related distortion in echo-planar imaging using EPI-based field maps. Magn. Reson. Med. 39 (2), 328–330. https://doi.org/10.1002/mrm.1910390223.

Robson, M.D., Anderson, A.W., Gore, J.C., 1997. Diffusion-weighted multiple shot echo planar imaging of humans without navigation. Magn. Reson. Med. 38 (1), 82–88. https://doi.org/10.1002/mrm.1910380113.

Romano, A., D'Andrea, G., Calabria, L.F., Coppola, V., Espagnet, C.R., Pierallini, A., Ferrante, L., Fantozzi, L., Bozzao, A., 2011. Pre- and intraoperative tractographic evaluation of corticospinal tract shift. Neurosurgery 69 (3), 696–705.

Schilling, K.G., Blaber, J., Hansen, C., Cai, L., Rogers, B., Anderson, A.W., Landman, B.A., 2020. Distortion correction of diffusion weighted MRI without reverse phase-encoding scans or field-maps. PLoS ONE 15 (7), e0236418.

Schilling, K.G., Blaber, J., Huo, Y., Newton, A., Hansen, C., Nath, V., Shafer, A.T., Williams, O., Resnick, S.M., Rogers, B., Anderson, A.W., Landman, B.A., 2019. Synthesized b0 for diffusion distortion correction (Synb0-DisCo). Magn. Reson. Imaging 64, 62–70.

Schilling, K.G., Rheault, F., Petit, L., Hansen, C.B., Nath, V., Yeh, F.C., ... Descoteaux, M., 2021. Tractography dissection variability: What happens when 42 groups dissect 14 white matter bundles on the same dataset? *Neuroimage, 243*, 118502. doi:10.1016/j.neuroimage.2021.118502.

Schmidt, C.F., Degonda, N., Luechinger, R., Henke, K., Boesiger, P., 2005. Sensitivity-encoded (SENSE) echo planar fMRI at 3T in the medial temporal lobe. Neuroimage 25 (2), 625–641. https://doi.org/10.1016/j.neuroimage.2004.12.002.

Shahar, T., Rozovski, U., Marko, N.F., Tummala, S., Ziu, M., Weinberg, J.S., Rao, G., Kumar, V.A., Sawaya, R., Prabhu, S.S., 2014. Preoperative imaging to predict intraoperative changes in tumor-to-corticospinal tract distance: an analysis of 45 cases using high-field intraoperative magnetic resonance imaging. Neurosurgery 75 (1), 23–30.

Skare, S., Bammer, R., 2010. *Jacobian weighting of distortion corrected EPI data.* Paper presented at the Proc. ISMRM, 5063.

Smith, S.M., Jenkinson, M., Woolrich, M.W., Beckmann, C.F., Behrens, T.E., Johansen-Berg, H., ... Matthews, P.M., 2004. Advances in functional and structural MR image analysis and implementation as FSL. *Neuroimage, 23 Suppl 1*, S208-219. doi:10.1016/j.neuroimage.2004.07.051.

Sotiropoulos, S.N., Jbabdi, S., Xu, J., Andersson, J.L., Moeller, S., Auerbach, E.J., Glasser, M.F., Hernandez, M., Sapiro, G., Jenkinson, M., Feinberg, D.A., Yacoub, E., Lenglet, C., Van Essen, D.C., Ugurbil, K., Behrens, T.E.J., 2013. Advances in diffusion MRI acquisition and processing in the Human Connectome Project. Neuroimage 80, 125–143.

Studholme, C., Constable, R.T., Duncan, J.S., 2000. Accurate alignment of functional EPI data to anatomical MRI using a physics-based distortion model. IEEE Trans. Med. Imaging 19 (11), 1115–1127. https://doi.org/10.1109/42.896788.

Tao, R., Fletcher, P.T., Gerber, S., Whitaker, R.T., 2009. A variational image-based approach to the correction of susceptibility artifacts in the alignment of diffusion weighted and structural MRI. Inf. Process Med. Imaging 21, 664–675. https://doi.org/10.1007/978-3-642-02498-6_55.

Tellez-Zenteno, J.F., Dhar, R., Wiebe, S., 2005. Long-term seizure outcomes following epilepsy surgery: a systematic review and meta-analysis. Brain 128 (Pt 5), 1188–1198. https://doi.org/10.1093/brain/awh449.

Tournier, J.D., Mori, S., Leemans, A., 2011. Diffusion tensor imaging and beyond. Magn. Reson. Med. 65 (6), 1532–1556. https://doi.org/10.1002/mrm.22924.

Tournier, J.D., Smith, R., Raffelt, D., Tabbara, R., Dhollander, T., Pietsch, M., . . . Connelly, A., 2019. MRtrix3: A fast, flexible and open software framework for medical image processing and visualisation. *Neuroimage, 202*, 116137. doi:10.1016/j.neuroimage.2019.116137.

Treiber, J.M., White, N.S., Steed, T.C., Bartsch, H., Holland, D., Farid, N., ... Chen, C.C., 2016. Characterization and Correction of Geometric Distortions in 814 Diffusion Weighted Images. *PLoS One, 11*(3), e0152472. doi:10.1371/journal.pone.0152472.

Tuch, D.S., Reese, T.G., Wiegell, M.R., Makris, N., Belliveau, J.W., Wedeen, V.J., 2002. High angular resolution diffusion imaging reveals intravoxel white matter fiber heterogeneity. Magn. Reson. Med. 48 (4), 577–582. https://doi.org/10.1002/mrm.10268.

Veraart, J., Fieremans, E., Novikov, D.S., 2016a. Diffusion MRI noise mapping using random matrix theory. Magn. Reson. Med. 76 (5), 1582–1593. https://doi.org/10.1002/mrm.26059.

Veraart, J., Novikov, D.S., Christiaens, D., Ades-Aron, B., Sijbers, J., Fieremans, E., 2016b. Denoising of diffusion MRI using random matrix theory. Neuroimage 142, 394–406. https://doi.org/10.1016/j.neuroimage.2016.08.016.

Veraart, J., Sijbers, J., Sunaert, S., Leemans, A., Jeurissen, B., 2013. Weighted linear least squares estimation of diffusion MRI parameters: strengths, limitations, and pitfalls. Neuroimage 81, 335–346. https://doi.org/10.1016/j.neuroimage.2013.05.028.

Wang, Y., Ma, X., Zhang, Z., Dai, E., Jeong, H.-K., Xie, B., Yuan, C., Guo, H., 2018. A comparison of readout segmented EPI and interleaved EPI in high-resolution diffusion weighted imaging. Magn. Reson. Imaging 47, 39–47.

Wasserthal, J., Neher, P., Maier-Hein, K.H., 2018. TractSeg - Fast and accurate white matter tract segmentation. Neuroimage 183, 239–253. https://doi.org/10.1016/j.neuroimage.2018.07.070.

Wu, M., Chang, L.C., Walker, L., Lemaitre, H., Barnett, A.S., Marenco, S., Pierpaoli, C., 2008. Comparison of EPI distortion correction methods in diffusion tensor MRI using a novel framework. Med. Image Comput. Comput. Assist Interv. 11 (Pt 2), 321–329. https://doi.org/10.1007/978-3-540-85990-1_39.

Yang, J.Y., Beare, R., Seal, M.L., Harvey, A.S., Anderson, V.A., Maixner, W.J., 2017. A systematic evaluation of intraoperative white matter tract shift in pediatric epilepsy surgery using high-field MRI and probabilistic high angular resolution diffusion imaging tractography. J. Neurosurg. Pediatr. 19 (5), 592–605. https://doi.org/10.3171/2016.11.PEDS16312.

Yang, J.-M., Beare, R., Wu, M.H., Barton, S.M., Malpas, C.B., Yeh, C.-H., Harvey, A.S., Anderson, V., Maixner, W.J., Seal, M., 2019. Optic Radiation Tractography in Pediatric Brain Surgery Applications: A Reliability and Agreement Assessment of the Tractography Method. Front. Neurosci. 13 https://doi.org/10.3389/fnins.2019.01254.

Yang, J.Y., Menon, R., Barton, S., Mandelstam, S.A., Kerr, R., Wrennall, J., ... Harvey, A.S., 2020. *One-stage, language-dominant, opercular-insular epilepsy surgery with multimodal structural and functional neuroimaging evaluation.* Paper presented at the Proc. ISMRM, 234.

Yang, J.-M., Yeh, C.-H., Poupon, C., Calamante, F., 2021. Diffusion MRI tractography for neurosurgery: the basics, current state, technical reliability and challenges. Phys. Med. Biol. 66 (15), 15TR01.

Yeh, F.C., Irimia, A., Bastos, D.C.A., Golby, A.J., 2021. Tractography methods and findings in brain tumors and traumatic brain injury. Neuroimage 245, 118651. https://doi.org/10.1016/j.neuroimage.2021.118651.